[CANCER RESEARCH 63, 5940–5949, September 15, 2003]

Reactive Oxygen Species-dependent c-Jun NH_2-terminal Kinase/c-Jun Signaling Cascade Mediates Neuroblastoma Cell Death Induced by Diallyl Disulfide[1]

Giuseppe Filomeni, Katia Aquilano, Giuseppe Rotilio, and Maria R. Ciriolo[2]

Department of Biology, University of Rome "Tor Vergata" via della Ricerca Scientifica, 00133 Rome [K. A., G. R., M. R. C.], and Department of Biomedical Sciences, University of Chieti "G. D'Annunzio" via dei Vestini, 66013 Chieti [G. F.], Italy

ABSTRACT

The pharmacological properties of garlic and its derivatives are long known, and their underling mechanisms are being extensively investigated. In this study we have addressed the effects of diallyl disulfide (DADS), an oil-soluble garlic molecule, on cell growth of neuroblastoma cell SH-SY5Y, focusing on the redox events associated with this compound. Treatment of SH-SY5Y cells with DADS resulted in arrest of cell cycle in G_2/M phase and commitment to apoptosis through the activation of the mitochondrial pathway (Bcl-2 down-regulation, cytochrome *c* release into the cytosol, and activation of caspase-9 and caspase-3). The earliest oxidative event observed after DADS treatment was the increase of production of reactive oxygen species, which reached the maximum yield on 30 min of DADS treatment. The oxidative burst resulted in protein and lipid damage as demonstrated by protein carbonyl accumulation and lipid peroxidation. We demonstrated that apoptosis induction was highly dependent on the activation of the redox-sensitive c-Jun NH_2-terminal kinase (JNK)/c-Jun pathway. In particular, we established that DADS treatment induces JNK dissociation from glutathione *S*-transferase and its activation by phosphorylation. Moreover, treatment with JNK inhibitor I significantly reduced DADS-induced apoptosis and treatment with the spin trap 5,5′-dimethyl-1-pyrroline *N*-oxide or overexpression of the antioxidant enzyme copper, zinc superoxide dismutase, resulted in the inhibition of DADS-mediated toxicity through attenuation of JNK/c-Jun pathway activation.

Overall, the results suggest a pivotal role for oxidative stress in DADS-induced apoptosis and, taking into account that tumor cells are deficient in antioxidants, suggest a plausible utilization of this compound as an antiproliferative agent in cancer therapy.

INTRODUCTION

In the last years, the strategy of selectively killing tumor cells by the induction of apoptosis has been addressed extensively (1). Different from necrosis, apoptosis is a gene-programmed mode of cell death, and depends on the subsequent activation of different processes involving cellular districts alteration (*i.e.* plasmamembrane or mitochondria), protein phosphorylation (*i.e.* mitogen activated protein kinases or transcription factors), and gene transcription. This sequence of events ultimately leads to the proteolytic activation of cysteine proteases (caspases), which, in turn, catalyze the cleavage of the cellular macromolecules (protein and DNA).

Intracellular redox environment has been suggested to modulate several cellular processes such as gene regulation, cell differentiation, and cell death (2, 3). Many of these processes depend on the balance between the intracellular concentrations of pro-oxidant species, such as ROS,[3] and antioxidant compounds. By scavenging ROS, cellular enzymatic antioxidant defense decreases the risk of oxidative insult that could give rise to irreversible alterations of structure and function of cellular macromolecules. Many observations have suggested that redox unbalance could be involved in both induction and execution of apoptosis; in fact, ROS production might be associated with several events along apoptotic pathways. Among these, binding of death receptors to their ligands (*e.g.* tumor necrosis factor/tumor necrosis factor receptor and FasL/Fas; Refs. 4, 5), disruption of mitochondrial transmembrane potential (6), and loss of intracellular glutathione content (7, 8), represent some of the most investigated phenomena. Among cell death inducers, phytochemicals, such as polyphenols from tea and grape, or sulfur compounds from garlic extracts, were considered of paramount importance in cancer therapy and prevention (9–11), because they do not exert toxic effect on differentiated cells (12, 13).

DADS is an oil-soluble compound present at very high concentration in garlic extracts, and it has been demonstrated to exert an inhibitory effect on 3-hydroxy-3-methyl-glutaryl-CoA reductase by forming an internal protein disulfide bond and thereby stabilizing the inactive form of the enzyme (14). This effect, together with those exerted on squalene monooxygenase activity, could partially explain the beneficial and therapeutic action of DADS on hypertension and cardiovascular diseases (15). Moreover, it has been proposed that DADS is able to induce growth arrest and death in several tumor cell types (16, 17). Although its role as an antitumor agent has been established, the mechanisms underlying such cytotoxic effects are not completely understood. The most plausible hypothesis refers to its molecular structure (permeable disulfide molecule) and suggests that DADS may represent an oxidizing agent able to induce oxidative stress-mediated cell death. However, the involvement of a redox unbalance on DADS administration is controversial. *In vivo* experiments did not show any significant change in antioxidant molecule levels, and no alterations of either glutathione redox state or related enzymes activity was observed (18). Conversely, several studies demonstrated that DADS treatment is often associated with an increase in the intracellular reduced glutathione content, suggesting the presence of an oxidative stress-independent mechanism (19, 20). However, the way in which DADS induces cytotoxicity has not been understood thus far, and the potential mechanism through which its signal is transduced within the cell remains to be clarified as well.

The aim of this study was to dissect the mechanisms underlying DADS cytotoxicity in SH-SY5Y neuroblastoma cells. We demonstrated that DADS induces cell death via a redox-mediated process involving ROS production, which resulted in a transient oxidative damage to proteins and lipids, and to the activation of the JNK/c-Jun transduction pathway. On the basis of the results obtained, we propose that oxidative stress plays a crucial role in DADS cytotoxicity, especially in cells that possess a poor antioxidant defense such as tumor cells.

Received 4/7/03; revised 6/18/03; accepted 6/26/03.

The costs of publication of this article were defrayed in part by the payment of page charges. This article must therefore be hereby marked *advertisement* in accordance with 18 U.S.C. Section 1734 solely to indicate this fact.

[1] Supported in part by grants from MIUR, Consiglio Nazionale delle Ricerche, Ministero della Sanità "Progetto di Ricerca Finalizzata," The Italian Association for Cancer Research (AIRC) and FIRB.

[2] To whom requests for reprints should be addressed, at Department of Biology, University of Rome "Tor Vergata," Via della Ricerca Scientifica, 1-00133 Rome, Italy. Phone: 39-06-7259-4374; Fax: 39-06-7259-4311; E-mail: ciriolo@bio.uniroma2.it.

[3] The abbreviations used are: ROS, reactive oxygen species; DADS, diallyl disulfide; JNK, c-Jun-NH_2-terminal kinase; Cu,Zn SOD, copper zinc superoxide dismutase; DCFDA, 2′-7′-dichlorodihydrofluorescein diacetate; DMPO, 5,5′-dimethyl-1-pyrroline *N*-oxide; MDA, malondialdehyde; 4-HNE, 4-hydroxynonenal; GST, glutathione *S*-transferase; MAP, mitogen-activated protein; hSOD, SH-SY5Y cells transfected with Cu,Zn SOD; DNP, 2,4-dinitrophenylhydrazine.

MATERIALS AND METHODS

Cell Culture

Human neuroblastoma cells SH-SY5Y were purchased from the European Collection of Cell Culture and grown in DMEM-F12 medium supplemented with 15% FCS, at 37°C in an atmosphere of 5% CO_2 in air. Monoclonal cell lines transfected with human wild-type Cu,Zn SOD (named hSOD) were obtained as described previously (21). Cells were routinely trypsinized and plated at 2×10^5/5-cm^2 flasks. Cell viability was assessed by trypan blue exclusion.

Treatments

Fifty mM solution of DADS (Sigma Co., St. Louis, MO) was prepared just before the experiments dissolving 5.5 M DADS in DMSO. Treatments were performed with different amounts of DADS ranging from 10 to 100 μM at 37°C in medium supplemented with serum. The concentration of 50 μM DADS was selected for all of the experiments, because this concentration gives a valuable degree of apoptosis at the times selected, and because it is in the range used for *in vivo* study (22). As control, equal amount of DMSO (0.1%) was added to untreated cells.

Detection of intracellular ROS was performed by a prior incubation of cells with 50 μM DCF-DA (Molecular Probes, Eugene, OR; dissolved in DMSO) for 30 min at 37°C (23) followed by treatment with DADS. Treatment with 100 μM *tert*-butyl hydroperoxide was used as a positive control.

Treatment with DMPO (Sigma Co.) was performed at a concentration of 15 mM, which under our experimental conditions does not result in toxicity. It was added 30 min before the addition of DADS and maintained throughout the experiment.

Treatment with the cell permeable JNK inhibitor I (Calbiochem-Novabiochem, La Jolla, CA) was performed at concentration of 10 μM, because lower concentrations did not show significant inhibition of c-Jun phosphorylation, and higher concentrations were toxic. JNK inhibitor I was added 1 h before the addition of DADS and maintained throughout the experiment.

Analysis of Cell Viability and Apoptosis

Adherent apoptotic cells were detected with the fluorescence microscope directly on chamber slides by analyzing the nuclear fragmentation after staining with Hoechst 33342 (Calbiochem-Novabiochem) dye as described previously (24). Alternatively, adherent (after trypsinization) and detached cells were combined, washed in PBS, and stained with 50 μg/ml propidium iodide before analysis by a FACScalibur instrument (Becton Dickinson, San Josè, CA). The percentages of apoptotic cells are evaluated according to Nicoletti *et al.* (25) by calculating peak area of hypodiploid nuclei.

Phosphatidylserine externalization was detected with the fluorescence microscope directly on chamber slides by analyzing the membrane fluorescence after staining with the impermeant dye Annexin V-FITC (Bender MedSystems, Vienna, Austria). Before image capture, propidium iodide was added to the monolayers to exclude necrotic cells.

Preparation of Cell Lysates and Western Blot Analyses

Cytosolic Caspase-9, Cytochrome C, and β-Actin Determination. Cells were washed with PBS and collected by centrifugation at $700 \times g$ for 5 min at 4°C. The cell pellet was resuspended in extraction buffer containing 220 mM mannitol, 68 mM sucrose, 50 mM PIPES-KOH (pH 7.4), 50 mM KCl, 5 mM EGTA, 2 mM $MgCl_2$, 1 mM DTT, and protease inhibitors (Sigma Co.) and treated as reported previously (24). Fifty μg of cytosolic protein extracts were loaded onto each lane of a 12% SDS-polyacrylamide gel, separated, and then blotted to nitrocellulose membrane (Bio-Rad, Hercules, CA). Mouse anticytochrome *c* (Clone 7H8.2c12; SIGMA Co.), anticaspase-9 (Clone 96-2-22; Upstate Biotechnology, Lake Placid, NY), and anti-β-actin (Clone AC-40; Sigma Co.) monoclonal antibodies were used as primary antibodies (1:5,000). The specific protein complex formed on appropriate secondary antibody (Bio-Rad) treatment (1:10,000) was identified using the "SuperSignal" substrate chemiluminescence reagent (Pierce, Rockford, IL).

Other Western Blot Analyses. Cell pellet was resuspended in lysis buffer containing 10 mM Tris-HCl (pH 7.4), 5 mM EDTA, 150 mM NaCl, 0.5% IGEPAL CA-630, and protease inhibitors (Sigma Co.). After 30-min incubation on ice, cells were disrupted by 10-s sonication. Lysates were then centrifuged at $14,000 \times g$ for 15 min at 4°C, and supernatants were removed and stored at −80°C. Twenty μg (for Cu,Zn SOD and Bcl-2) or 50 μg (for c-Jun, JNK, GST-π-1, and β-actin) of proteins were loaded on 12% polyacrylamide gel and transferred onto a nitrocellulose membrane. Polyclonal anti-Cu,Zn SOD (1:2000); anti-GST-π-1 (1:1000); anti-c-Jun and anti-JNK (1:200) or monoclonal anti-phospho-activated c-Jun and JNK isoforms (1:200; Santa Cruz Biotechnology, Santa Cruz, CA); and anti-Bcl-2 and β-actin (1:5000; Sigma Co.) were used as primary antibodies.

Immunoprecipitation

Cell pellet was resuspended in lysis buffer, and after 30-min incubation on ice, cells were disrupted by 10-s sonication. Lysates were then centrifuged at $14,000 \times g$ for 15 min at 4°C. Three-hundred μg of protein were incubated in lysis buffer with 10 μl of anti-JNK antibody to a total volume of 300 μl for 2 h at 4°C. Immunocomplexes were absorbed with 20 μl of protein A-Sepharose for 30 min at 4°C. After three washes with lysis buffer, immune pellets were boiled in SDS sample buffer. Fifty μg of proteins were loaded on 15% SDS-polyacrylamide gel and transferred to nitrocellulose. Polyclonal anti-GST-π-1 (Calbiochem-Novabiochem) antibody was used as primary antibody (1:200).

Enzyme Activities

Cu,Zn SOD activity was measured on cell lysates by a polarographic method as reported previously (26). Data were expressed as μg/mg protein with reference to purified human Cu,Zn SOD. Activity was also evidenced on nondenaturing 7.5% polyacrylamide gels by loading 50 μg of supernatant proteins. After electrophoresis, gel was stained as described previously (23).

Caspase 3 activity was monitored fluorometrically as described previously (24).

Measurement of Oxidative Damage

Carbonylated proteins were detected using the Oxyblot kit (Intergen, Purchase, NY). Briefly, 20 μg of proteins were reacted with DNP for 15 min at 25°C. Samples were resolved on 12% SDS-polyacrylamide gels, and DNP-derivatized proteins were identified by immunoblot using an anti-DNP antibody.

Levels of MDA and 4-HNE were measured by a colorimetric method using the Lipid Peroxidation Assay kit (Calbiochem-Novabiochem) according to manufacturer instructions. Lipid peroxidation was evaluated with reference to standard curves obtained with known amounts of MDA and 4-HNE, and expressed as μmol MDA +4-HNE/mg protein.

Proteins were determined by the method of Lowry *et al.* (27).

Data Presentation

All of the experiments were done at least six different times ($n = 5$) unless otherwise indicated. Data are expressed as means ± SD, and significance was assessed by Student's *t* test. Differences with *P*s <0.05 were considered significant.

RESULTS

DADS Induces Cell Cycle Arrest and Apoptosis in SH-SY5Y Cells. The effects of DADS on cell cycle of neuroblastoma cell, SH-SY5Y, were analyzed by performing cytofluorometric analyses. Fig. 1*A* shows that 50 μM DADS induced an increase of SH-SY5Y cells in G_2/M phase after 12 h of treatment, reaching values of 42.52%. After 24 h, the percentage of cell population that showed apoptotic features (sub-G_1 region) was ~30%, suggesting that the blockage in G_2/M phase finally results in the triggering of the apoptotic program. These results were additionally confirmed by fluorescence microscopy analyses of cell nuclei stained with the DNA-specific dye Hoechst 33342 and annexin V FITC. Fig. 1*B* shows that treatment with 50 μM DADS for 24 h induced chromatin condensation and nuclear fragmentation, which represent the final steps of apopto-

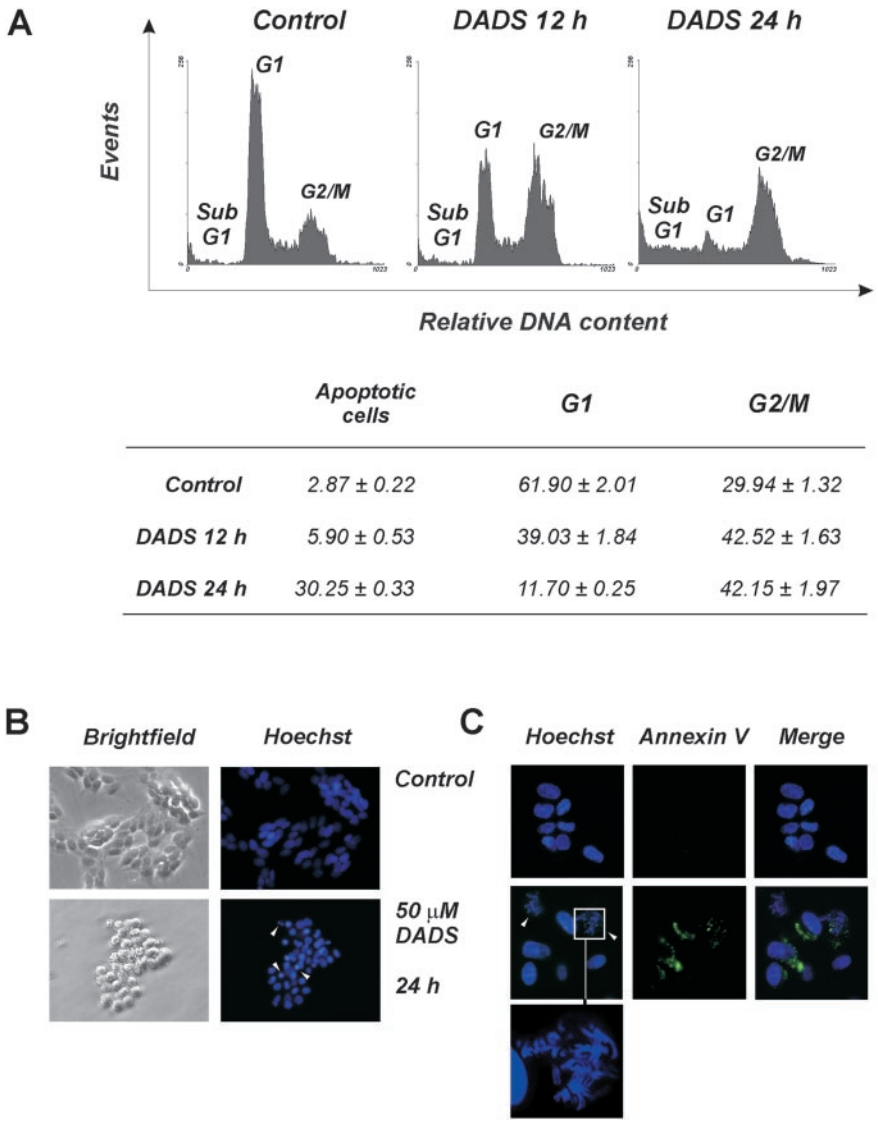

	Apoptotic cells	G1	G2/M
Control	2.87 ± 0.22	61.90 ± 2.01	29.94 ± 1.32
DADS 12 h	5.90 ± 0.53	39.03 ± 1.84	42.52 ± 1.63
DADS 24 h	30.25 ± 0.33	11.70 ± 0.25	42.15 ± 1.97

Fig. 1. DADS induces cell cycle arrest and apoptosis in SH-SY5Y cells. *A*, SH-SY5Y cells were treated with 50 μM DADS for 12 and 24 h, washed and stained with propidium iodide. Analysis of cell cycle and apoptosis was performed by a FACScalibur instrument, and percentages of staining-positive cells were calculated using WinMDI version 2.8 software. The cell cycle plots reported are from a typical experiment done in triplicate of five that gave similar results (sub-G_1, apoptotic cells). A table indicating the percentages of nuclei in the different phases of cell cycle is shown at the *bottom*. *B*, SH-SY5Y cells were grown on chamber-slides and treated for 24 h with 50 μM DADS. After washing with PBS, cells were stained with Hoechst 33342 and visualized by fluorescence microscopy. *White arrows* indicate fragmented nuclei. *C*, cells, treated with 50 μM DADS for 12 h were analyzed by fluorescence microscopy after staining with Hoechst 33342 and with annexin V-FITC. *White arrows* indicate metaphasic nuclei with discrete chromosomes: a detail is shown at the bottom.

sis. Fragmentation of nuclei was preceded by the translocation of phosphatydilserine from the inner to the outer side of the plasma membrane, which was significant at 12 h after treatment and concomitant with the appearance of a many metaphasic nuclei (Fig. 1*C*). The presence of discrete chromosomes, evidenced with ×400 magnification images, confirmed the increase of G_2/M-arrested cell number showed by FACS analyses (Fig. 1*A*).

DADS Induces the Execution of Apoptosis through the Activation of the Mitochondrial Pathway. To establish the sequence of events occurring during DADS-induced apoptosis, we measured some of the molecular markers involved in programmed cell death. Cytosolic extracts were prepared under conditions that keep mitochondria intact, and cytosolic cytochrome *c* protein levels were measured by immunoblot analysis. Fig. 2*A* shows that the cytosol from untreated SH-SY5Y cells contained no detectable amount of cytochrome *c*, whereas it became detectable after 6 h of 50 μM DADS treatment.

Hallmarks of the apoptotic process are the activation of cysteine proteases (caspases), which represent both initiators and executors of death signals. The activation of the upstream caspase-9 was evaluated by Western blot analysis of the appearance of the active proteolysed caspase band. Fig. 2*A* shows that active caspase-9 was not present in untreated cells, whereas it accumulated in a time-dependent manner in SH-SY5Y cells after treatment with 50 μM DADS. Proteolytic activity was also measured by testing the cytosolic extracts for their ability to cleave the fluorometric substrate Ac-DEVD-AFC, which is specific for caspase-3. Fig. 2*B* shows that the activity of caspase-3 in DADS-treated cells was significantly higher than control as early as 12 h after treatment.

Bcl-2 protein is regarded as a mitochondrial factor responsible for the decision between cell life and death, and it has been associated with the regulation of the intracellular redox state (28). Fig. 2*A* shows that, after 24 h treatment with 50 μM DADS, Bcl-2 expression levels decreased in SH-SY5Y total extracts, representing an additional hallmark of the toxic effect induced by DADS.

DADS Induces Oxidative Stress. On the basis of its chemical structure, characterized by two double bonds and by a disulfide bridge, DADS could represent a powerful alkylating and oxidizing agent leading to the production of reactive radicals. Therefore, we investigated the role of ROS as potential mediators of DADS-induced cytotoxicity in SH-SY5Y cells. Fig. 3*A* shows the production of ROS during the first 2 h of DADS treatment. SH-SY5Y cells underwent a dramatic increase of ROS flux as early as 15 min after DADS administration with a peak value at 30 min. These results implied a strict association between DADS effects and oxidative unbalance. To establish the occurrence of an oxidative stress on DADS treatment, we measured some molecular targets of increased ROS production. Be-

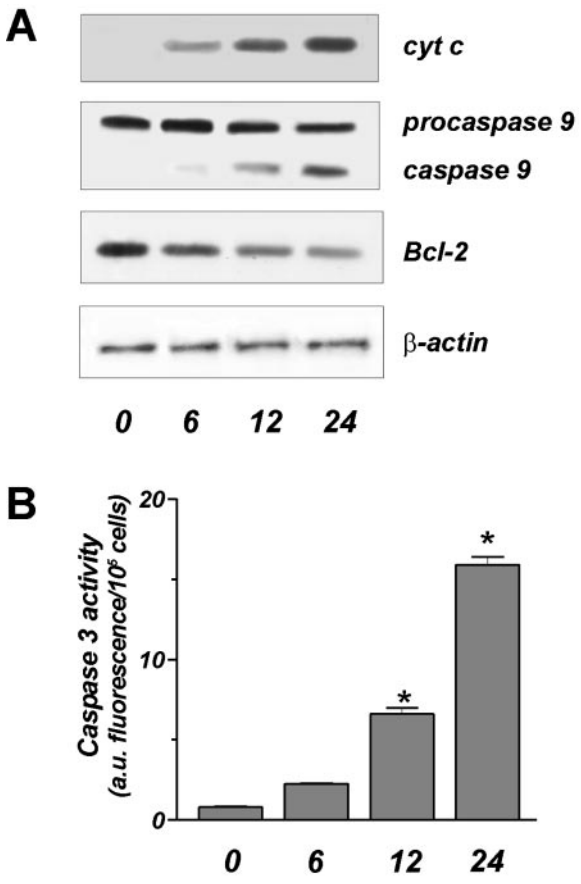

Fig. 2. DADS induces apoptosis through the activation of the mitochondrial pathway. *A*, SH-SY5Y cells were treated with 50 μM DADS for 24 h. Twenty μg of cytosolic extracts were loaded onto each lane for detection of cytochrome *c* or procaspase-9 and caspase-9 protein levels. Twenty μg of total cell extracts were loaded for detection of Bcl-2 expression levels. β-Actin was used as loading control. Immunoblots are from one experiment representative of three that gave similar results. *B*, caspase-3 activity was determined by a fluorimetric assay on cell extracts using the synthetic substrate Ac-DEVD-AFC. Data are shown as arbitrary units and expressed as mean; *bars*, $\pm$SD; $n = 4$ ($*$, $P < 0.001$).

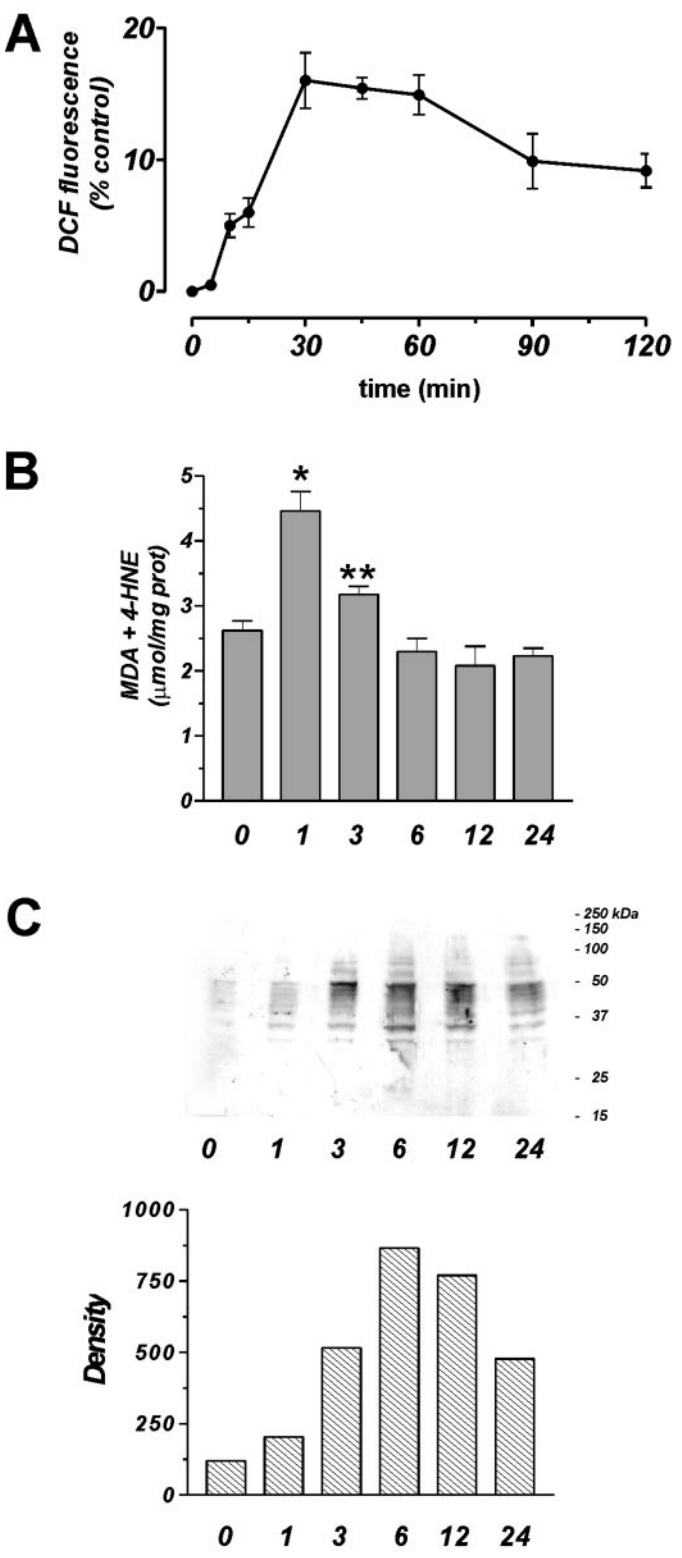

Fig. 3. DADS treatment induces ROS production and oxidative damage. *A*, SH-SY5Y cells were treated with 50 μM DADS up to 2 h, incubated with 50 μM DCF-DA at 37°C. At indicated time points, cells were washed with PBS, and ROS production was analyzed by FACScalibur instrument. Data are reported as mean; *bars*, $\pm$SD ($n = 5$). *B*, SH-SY5Y cells were treated with 50 μM DADS up to 24 h. Lipid peroxidation was evaluated by measuring the levels of MDA and 4-HNE using a colorimetric method. Data are expressed as means; *bars*, $\pm$SD ($n = 5$); $*$, $P < 0.001$, $**$, $P < 0.05$ *versus* untreated cells. *C*, protein carbonyls were identified upon derivatization with DNP followed by immunoblot using anti-DNP antibody. Twenty μg of derivatized proteins were loaded onto each lane. A representative immunoblot of three that gave similar results is shown (*top panel*). Densitometric analysis of each lane was calculated using Quantitiy One Software (Bio-Rad) and data are shown as arbitrary units (*bottom panel*).

cause of the presence of polyunsaturated phospholipids, cell membranes are susceptible to oxidative damage that can result in the formation of lipid peroxides. Fig. 3*B* shows a significant increase in the end products of lipid peroxidation, MDA and 4-HNE, after 1-h treatment with 50 μM DADS concomitantly with the massive production of ROS (Fig. 3*A*). Proteins represent another target of ROS that, for instance, can lead to the formation of carbonyl groups on particular amino acid residues. Fig. 3*C* shows that treatment with 50 μM DADS induced a significant increase of protein carbonyls, starting from 1 h and reaching the higher content between 6 and 12 h.

Antioxidants Counteract DADS-induced Oxidative Stress and Apoptosis. To additionally establish the role of oxidative stress as mediator of DADS-induced cellular cytotoxicity, we carried out experiments with SH-SY5Y transfected with the antioxidant enzyme Cu,Zn SOD (hSOD cells). Fig. 4*A* shows that hSOD cells had a significant increase in the expression and activity levels of Cu,Zn SOD. The transfection with Cu,Zn SOD resulted in a significant protection against DADS-induced ROS production (Fig. 4*B*). In particular, a valuable determination of ROS concentration was determined only on 15 min of treatment, and it corresponds to 20% of the highest value obtained with SH-SY5Y cells. This inhibition results in a significant decrement in oxidative damage of cellular macromolecules. Fig. 4*C* shows that the levels of carbonylated proteins slightly increased only after 6 h of treatment with 50 μM DADS, reaching a

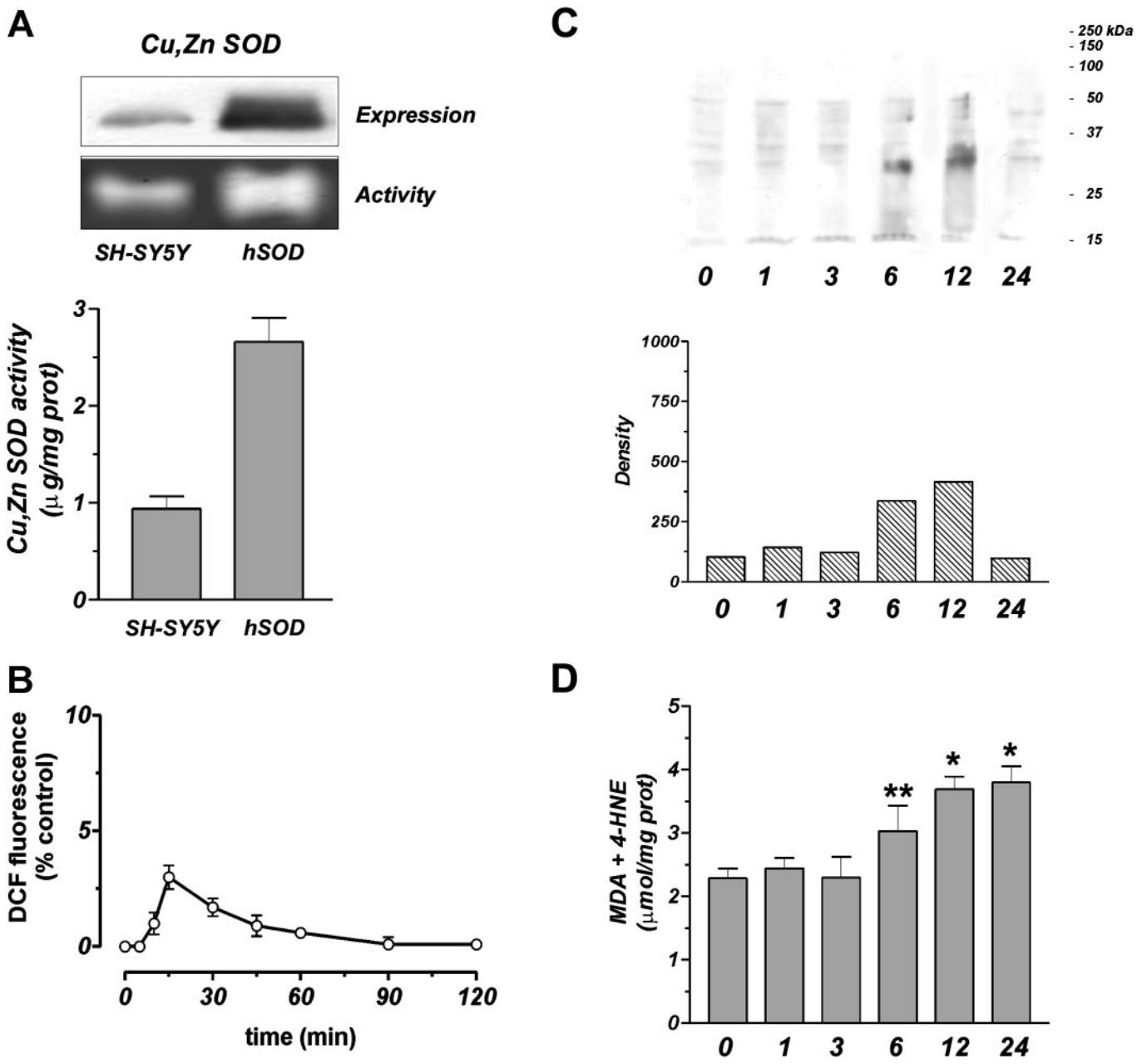

Fig. 4. Cu,Zn SOD overexpression protects against DADS-mediated oxidative damage. *A*, Cu,Zn SOD expression level was measured by Western blot analyses after loading 20 μg of total cell extracts. Cu,Zn SOD activity was detected on polyacrylamide gel by the NBT/riboflavin staining. Fifty μg of nondenatured proteins were loaded onto each lane. One experiment representative of three that gave similar results is shown. *Bottom panel*, polarographic assay of Cu,Zn SOD activity. *B*, hSOD cells were treated with 50 μM DADS up to 2 h, incubated with 50 μM DCF-DA at 37°C. At indicated time points, cells were washed with PBS and ROS production was analyzed by FACScalibur instrument as described in Fig. 3*A*. *C*, hSOD cells were treated with 50 μM DADS up to 24 h. Protein carbonyls were identified upon derivatization with DNP as described in Fig. 3*C*. *D*, lipid peroxidation was evaluated by measuring the levels of MDA and 4-HNE using a colorimetric method as described in Fig. 3*B*. Data are expressed as means; *bars*, $\pm$SD ($n = 5$); *, $P < 0.001$, **, $P < 0.05$ *versus* untreated cells.

maximum at 12 h. In particular, a different susceptibility to oxidation was observed in these cells, with the low molecular weight proteins being preferentially carbonylated with respect to the higher molecular weight components. Moreover, comparison of density plots, evaluated by a total scanning of each lane, showed a 50% reduction of carbonyl levels both at 6 and 12 h with respect to SH-SY5Y (Fig. 4*C*, *bottom panel*), confirming that the increased antioxidant power was able to buffer the oxidative insult mediated by DADS. This protective effect was also observed by measuring the levels of lipid peroxidation (Fig. 4*D*). The production of MDA and 4-HNE showed a different kinetic and a lower increase when compared with that observed in untransfected cells (Fig. 3*B*).

To establish whether the protective effect exerted by Cu,Zn SOD was operative also on DADS-induced apoptosis, we determined the distribution of hSOD cell population in the different phases of cell cycle after DADS treatment. Cytofluorimetric analyses demonstrated that hSOD cells were less susceptible to 50 μM DADS treatment and showed a delay in the activation of the events that characterized SH-SY5Y cell response (Fig. 5*A*). Cell cycle arrest was not evident at 12 h but started to become significant only after 24 h of treatment. Moreover, although on 24-h DADS treatment the cells in G_2/M phase were significantly higher than the control (45.63 ± 1.98 *versus* 28.87 ± 3.21), the percentage of cell population that shows apoptotic features (sub-G_1 region) remained at very low values (9.12 ± 0.67;

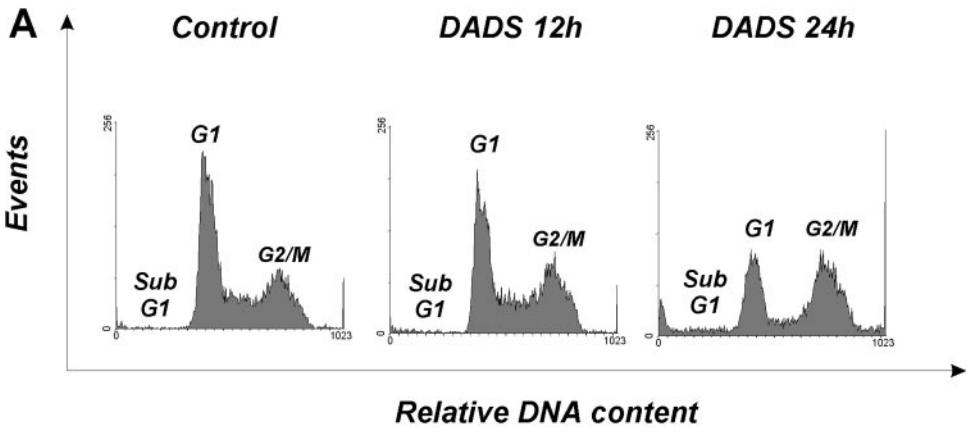

	Apoptotic cells	G1	G2/M
Control	3.45 ± 0.52	59.71 ± 2.15	28.87 ± 3.21
DADS 12 h	5.04 ± 0.73	51.55 ± 1.98	34.11 ± 2.97
DADS 24 h	9.12 ± 0.67	32.06 ± 2.18	45.63 ± 1.98

Fig. 5. Antioxidants counteract DADS-induced cell cycle arrest and apoptosis. *A*, hSOD cells were treated with 50 μM DADS for 12 and 24 h, washed with PBS, and stained with propidium iodide. Analysis of cell cycle and apoptosis was performed as described in Fig. 1*A*. *B*, SH-SY5Y cells were treated with 15 mM DMPO for 30 min before and maintained during treatment with 50 μM DADS (24 h). After treatment cells were stained with propidium iodide for cell cycle and apoptosis cytofluorimetric analyses. Percentages of apoptotic and G_2/M-arreted cells are expressed as means; *bars*, ±SD ($n = 5$); *, $P < 0.001$ *versus* DADS-treated cells.

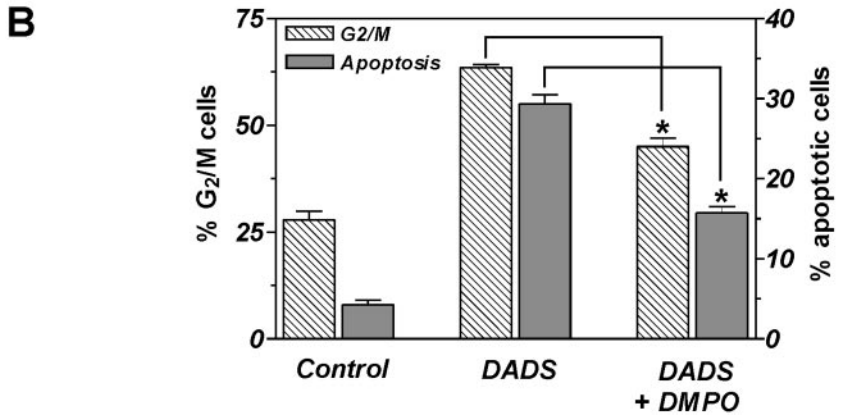

Fig. 5*A*). The same result was obtained on staining with Hoechst 33342 and annexin V, which showed undetectable annexin V-positive cells after 12 h and only a low amount of fragmented nuclei after 24 h of treatment (data not shown).

Spin trapping molecules could chemically prevent ROS-mediated oxidative damage, because they react efficiently with ROS preventing their propagation (29). Hence, we tested whether DMPO, a highly effective spin-trapping compound, could also exert a protective role against DADS-induced cell death by scavenging a broad range of ROS in parental SH-SY5Y cells. Cells were preincubated with 15 mM DMPO and treated with 50 μM DADS for 24 h. Fig. 5*B* shows that DMPO is able to significantly reduce the percentages of apoptotic and G_2/M-arrested cells confirming the strict relationship between ROS-mediated oxidative burst and apoptotic response.

DADS Treatment Affects GST-π-1/JNK Complex. Several papers of the last decade demonstrated that macromolecules, which belong to the family of MAP kinases, can be indirectly regulated in their activity by the alteration of intracellular redox environment (24, 30). Among MAP kinases, JNK has often been suggested to be a key modulator of the ROS-mediated signal transduction in many neuronal-derived cell lines (31, 32). For this reason, we decided to investigate the JNK-mediated pathway in SH-SY5Y cells after treatment with 50 μM DADS. Fig. 6*A* shows that GST-π-1, the inhibitory subunit of JNK, was reduced significantly after 6 and 12 h DADS treatment; however, by analyzing hSOD lysates, no changes in GST levels were detected. To assess whether the different levels of GST were related to the dissociation from JNK, cell lysates were immunoprecipitated with an anti-JNK polyclonal antibody and used for Western blot analyses. Fig. 6*B* shows that the amount of immunoprecipitated JNK was not significantly altered; on the contrary, the amount of GST that coprecipitates with JNK changed significantly throughout the experimental time points analyzed. In particular, the formation of GST/JNK complex was inhibited at 1 h DADS treatment (−79%), remained at low values at 3 h (−48%), and reached control levels after 6 h of treatment. The kinetics of binding paralleled ROS burst (Fig. 3*A*), suggesting a direct relationship between DADS-mediated oxidative alteration and JNK activation. Moreover, immunoprecipitation analyses performed with hSOD cell lysates showed that capacity of GST to bind JNK was less affected by DADS at 1 h

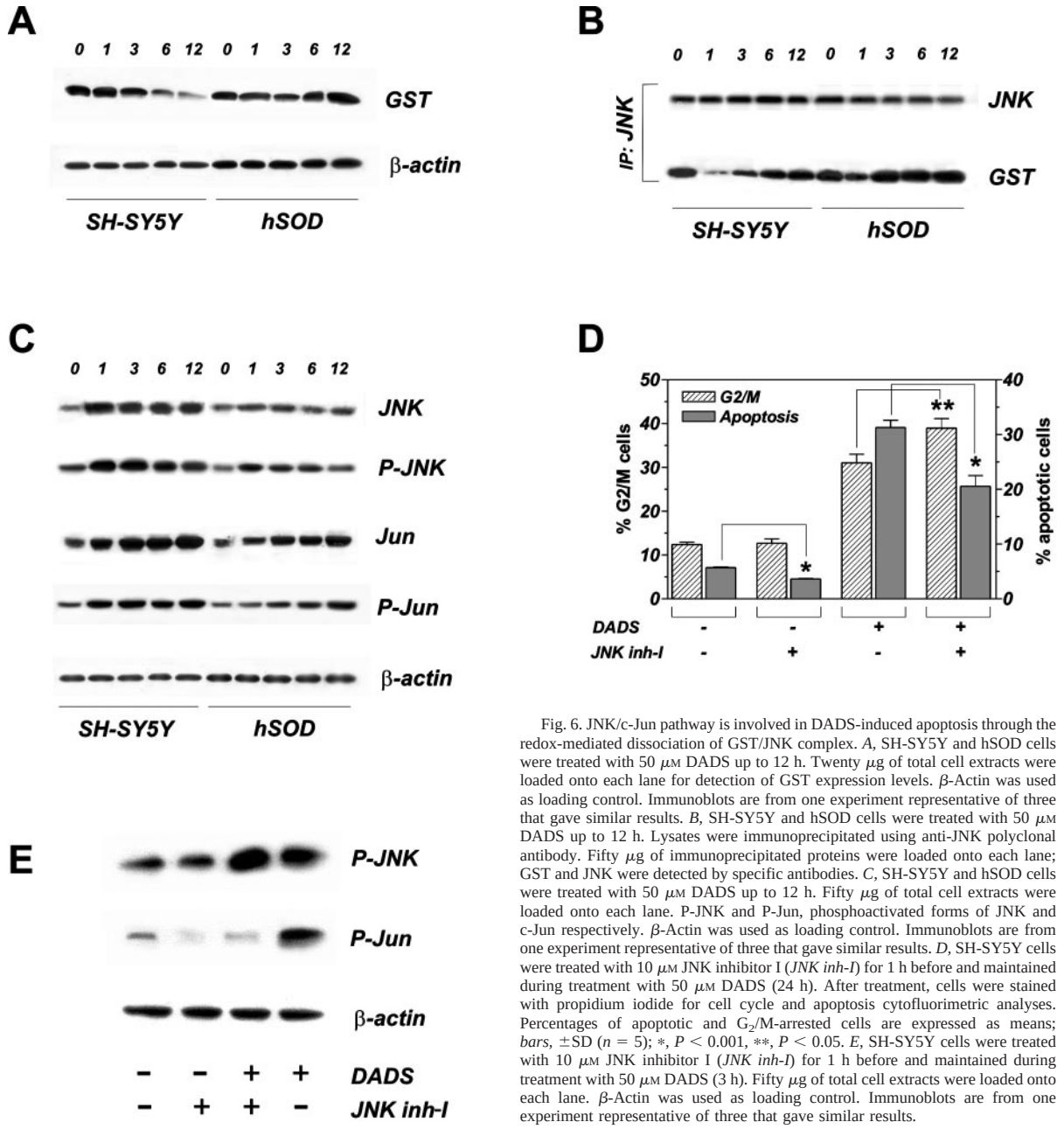

Fig. 6. JNK/c-Jun pathway is involved in DADS-induced apoptosis through the redox-mediated dissociation of GST/JNK complex. *A*, SH-SY5Y and hSOD cells were treated with 50 μM DADS up to 12 h. Twenty μg of total cell extracts were loaded onto each lane for detection of GST expression levels. β-Actin was used as loading control. Immunoblots are from one experiment representative of three that gave similar results. *B*, SH-SY5Y and hSOD cells were treated with 50 μM DADS up to 12 h. Lysates were immunoprecipitated using anti-JNK polyclonal antibody. Fifty μg of immunoprecipitated proteins were loaded onto each lane; GST and JNK were detected by specific antibodies. *C*, SH-SY5Y and hSOD cells were treated with 50 μM DADS up to 12 h. Fifty μg of total cell extracts were loaded onto each lane. P-JNK and P-Jun, phosphoactivated forms of JNK and c-Jun respectively. β-Actin was used as loading control. Immunoblots are from one experiment representative of three that gave similar results. *D*, SH-SY5Y cells were treated with 10 μM JNK inhibitor I (*JNK inh-I*) for 1 h before and maintained during treatment with 50 μM DADS (24 h). After treatment, cells were stained with propidium iodide for cell cycle and apoptosis cytofluorimetric analyses. Percentages of apoptotic and G_2/M-arrested cells are expressed as means; *bars*, $\pm$SD ($n = 5$); *, $P < 0.001$, **, $P < 0.05$. *E*, SH-SY5Y cells were treated with 10 μM JNK inhibitor I (*JNK inh-I*) for 1 h before and maintained during treatment with 50 μM DADS (3 h). Fifty μg of total cell extracts were loaded onto each lane. β-Actin was used as loading control. Immunoblots are from one experiment representative of three that gave similar results.

(−34%), and it was restored efficiently during the following time points examined.

DADS Induces the Activation of JNK/Jun Pathway. The activated form of JNK (phospho-JNK) mediates the phosphoactivation of c-Jun, thus regulating the transcription of several genes involved in cell proliferation or death. Fig. 6*C* shows Western blot analyses of basal and phosphorylated isoforms of both c-Jun and the upstream kinase JNK-1 on treatment with 50 μM DADS. Phospho-JNK was rapidly detected after 1 h of treatment and slowly decreased until 12 h on DADS addition, although it remained at very high levels. This event was followed by a rapid and stable phosphoactivation of c-Jun, which started to be evident as soon as after 1 h and was maintained at high levels until phosphatidylserine was externalized (12 h). On the contrary, hSOD cells showed a significantly lower activation of this pathway, enforcing the hypothesis that, in our experimental system, JNK/c-Jun-mediated signal transduction was a ROS-dependent event. The observed changes in the levels of activated isoforms were paralleled by the expression levels of total c-Jun and JNK (Fig. 6*C*). The involvement of JNK/c-Jun pathway in DADS-mediated toxicity was confirmed by the experiments carried out with the cell-permeable JNK inhibitor I. Fig. 6*D* shows that treatment of cells with 10 μM of JNK inhibitor I protects from DADS-induced apoptosis. In particular, we observed a 30% reduction in apoptotic cells and a considerable rise of cells in G_2/M phase. The efficacy of inhibition of JNK kinase activity was additionally evaluated by Western blot analyses of the phosphoactivated form of c-Jun. Fig. 6*E* shows that 3 h of DADS treatment performed in the presence of JNK inhibitor I was not able to induce phosphorylative modification of c-Jun, although a larger amount of phospho-JNK was still present.

DISCUSSION

During the last few years, several papers on tumor-preventive and therapeutic action of garlic and its derivatives have been reported.

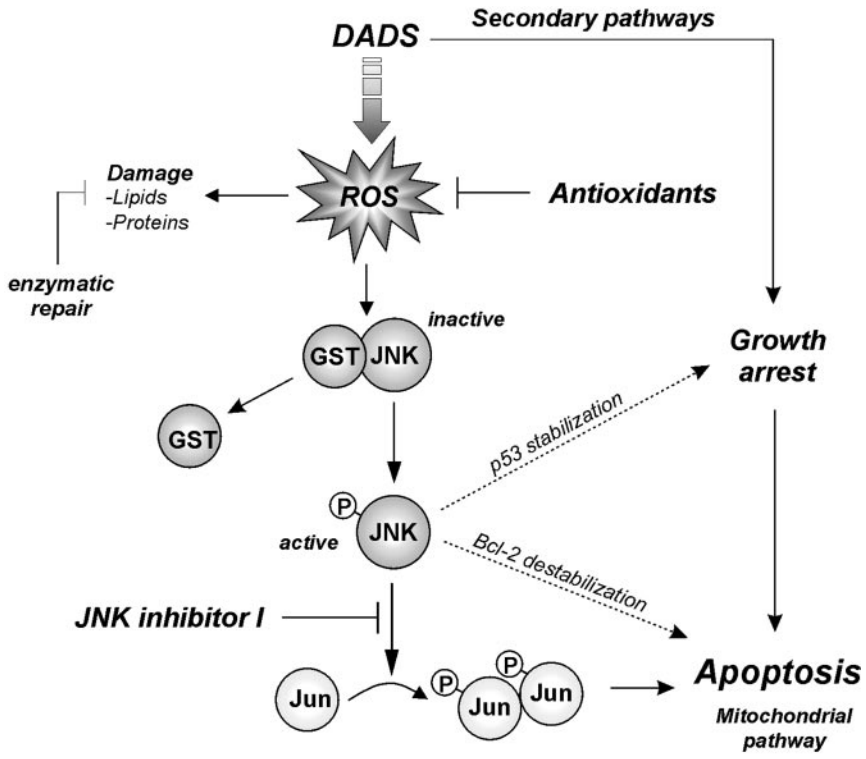

Fig. 7. Schematic model for DADS-induced cell death.

Many putative cellular targets for these compounds have been hypothesized in such a way as to establish a mechanism that selectively kills tumor cells. Among garlic derivatives, DADS represents the majority (60%) of oil-soluble compounds, and it has been demonstrated to induce cell cycle arrest and apoptosis in cultured cell lines, such as leukemia HL-60 (16) and colon carcinoma HT-29 (17). However, the molecular mechanism for its therapeutic action as an antitumor agent has not been clarified yet.

In the present report we demonstrated that DADS induces growth arrest and apoptosis in the neuroblastoma cell line SH-SY5Y through the activation of the canonical mitochondrial pathway (Bcl-2 downregulation, cytochrome *c* release into the cytosol, and activation of caspase-9 and caspase-3). ROS production represents the earliest step in the scale of events occurring on DADS treatment, as it was observed during the first 15 min. The oxidative burst resulted in membrane and protein damage; however, whereas lipid peroxide concentrations rapidly decreased to control values, mirroring the kinetics of ROS burst, the rate of protein carbonyls remained at very high levels until 12 h of treatment. These results suggest a 2-fold action for DADS-mediated oxidative stress: (*a*) rapid and massive burst of oxyradicals injuring phospholipids that were efficiently recovered by enzymatic antioxidant defense; and (*b*) prolonged and sustained oxidative damage injuring specific amino acid residues that were not so efficiently cleaned up by cellular "repair machineries." The involvement of ROS-mediated damage during the early phases of DADS cytotoxic action was additionally established by using the antioxidant spin-trap DMPO, which was able to efficiently inhibit cell cycle arrest and apoptosis. Moreover, experiments carried out with hSOD cells demonstrated that, by supplying cells with a more efficient antioxidant power, DADS cytotoxicity was almost completely counteracted. As expected, such protection was linked with a complete inhibition of oxidative injuries and damages on target molecules at early times of treatment. However, the evidence of an increased lipid peroxidation at 12 h and 24 h, along with a different pattern of protein carbonyls, suggests that these molecules could also represent a secondary target of DADS cytotoxicity. In fact, although transfection with Cu,Zn SOD resulted in an almost complete inhibition of ROS burst and a significant delay of the cytostatic effects induced by DADS, it was not sufficient to impede the observed late alteration in cell cycle progression. Therefore, other different modes of action should be taken into account in the cascade of events leading to cell death, such as histones acetylation (33, 34), inactivation of p34(cdc2) kinase activity (35, 36), inhibition of membrane association of tumoral p21H-ras (37, 38), and a plausible widespread thiol oxidizing action.

The results thus far discussed confirmed a role for ROS in the induction of cell death and suggested the involvement of a redox-signaling pathway linking the two events. Among redox-sensitive factors able to modulate cell cycle progression, MAP kinases are known to be activated in response to environmental stress such as exposure to UV (30), hyperosmotic conditions (39), and modulated by ROS production (24). In particular, neural cell death is often mediated by the activation of JNK, the c-Jun upstream MAP kinase (40). Usually, at physiological conditions, the basal activity of JNK is maintained low through the formation of an heterocomplex with GST-π-1. In fact, besides its established role as a detoxifying enzyme, GST-π-1 is able to bind JNK and inhibit its kinase activity limiting the degree of c-Jun phosphorylation (31, 41). Upon stress condition, GST and JNK dissociate leading to JNK activation and formation of dimers and/or multimers of GST by disulfide bridges (41). Similarly, in SH-SY5Y cells, we found that DADS treatment induces a rapid dissociation of GST from JNK (1 h). As a result, the phopshoactivation of JNK and c-Jun were observed confirming a strict relationship between the two events. However, although JNK protein levels increase during DADS treatment, a decrease in GST levels was evidenced at 6 h, far away from the phosphoactivation of JNK. This could be explained in terms of a degradative process affecting GST after JNK dissociation. In fact, it has been suggested that oxidatively modified GST, which has lost the engagement with JNK, is efficiently proteolyzed (41).

The results obtained with hSOD cells indicated that, by quenching ROS burst, the activation of JNK and c-Jun were significantly inhibited. In particular, the phosphorylative cascade induced by JNK was turned off at 12 h, when a high concentration of phospho-JNK was still detected in SH-SY5Y cells. Furthermore, it is noteworthy that in hSOD cells the levels of the phosphoactivated forms of JNK and c-Jun were significantly lower than untransfected cells.

The involvement of JNK/c-Jun pathway in DADS-induced apoptosis was strengthened by the experiments carried out in the presence of cell-permeable JNK inhibitor I, a synthetic peptide able to specifically block JNK-mediated c-Jun phosphorylation without interfering with other pathways, such as those dependent on ERK or other stress activated protein kinases. The data obtained in our study coincide with the suggested primary role played by JNK in the induction of apoptosis in neural-derived cells. In fact, SH-SY5Y cells treated only with the JNK inhibitor I showed a significant reduction of spontaneous apoptotic cell death (5.91 ± 0.62 *versus* 3.22 ± 0.50). This protective effect was also obtained on treatment with DADS; in particular, by blocking c-Jun phosphorylation, a decrease in the percentage of apoptotic cells (-32%) was observed. Moreover, the results obtained with JNK inhibitor I were different from those evidenced on treatment with DMPO, in which the rate of both apoptotic and growth-arrested cells declined. This effect could be explained because the selective blockage of c-Jun phosphoactivation was able to inhibit apoptosis execution but not cell cycle arrest, which, on the other hand, represent an upstream ROS-dependent event. In addition, it has been demonstrated that JNK is efficient in phosphoactivating other target proteins involved in the induction of cell cycle arrest. Among these, a pivotal role could be played by p53 for which it has been suggested a specific JNK-mediated phosphorylation on thr-81 to inhibit ubiquitination process and activate its transcriptional activities in response to stress (42). Despite this function, JNK might enable apoptosis by interfering directly with mitochondria, resulting in release of cytochrome *c* (43) through destabilization of members of the Bcl-2 family (44, 45). Indeed, the observed down-regulation of Bcl-2 in our experimental model could also be the result of JNK activation. Therefore, the partial recovery from apoptosis and the increase in G_2/M phase, by treatment with JNK inhibitor I confirmed the existence of more than one pathway through which JNK functions (45). On the basis of previous and current findings, we schemed a simplified model for DADS-induced apoptosis in SH-SY5Y cells (Fig. 7).

Overall the results shed light on the molecular mechanisms responsible for DADS cytotoxicity and give additional effort to the studies carried out to assess a potential antitumor effect for garlic. This could be fundamental to postulate a preventive use of a garlic-enriched diet and/or to program a therapeutic approach with its derivatives in cancer therapy.

REFERENCES

1. Ferreira, C. G., Epping, M., Kruyt, F. A., and Giaccone, G. Apoptosis: target of cancer therapy. Clin. Cancer Res., *8:* 2024–2034, 2002.
2. Buttke, T. M., and Sandstrom, P. A. Oxidative stress as mediator of apoptosis. Immunol. Today, *15:* 7–10, 1994.
3. Wang, X., Martindale, J. L., Liu, Y., and Holbrook, N. J. The cellular response to oxidative stress: influences of mitogen-activated protein kinase signalling pathways on cell survival. Biochem. J., *333:* 291–300, 1998.
4. Carmody, R. J., and Cotter, T. G. Signalling apoptosis: a radical approach. Redox Rep., *6:* 77–90, 2001.
5. Gouaze, V., Andrieu-Abadie, N., Cuvillier, O., Malagarie-Cazenave, S., Frisach, M. F., Mirault, M. E., and Levade, T. Glutathione peroxidase-1 protects from CD95-induced apoptosis. J. Biol. Chem., *277:* 42867–42874, 2002.
6. Ricci, J. E., Gottlieb, R. A., and Green, D. R. Caspase-mediated loss of mitochondrial function and generation of reactive oxygen species during apoptosis. J. Cell Biol., *160:* 65–75, 2003.
7. Ghibelli, L., Fanelli, C., Rotilio, G., Lafavia, E., Coppola, S., Colussi, C., Civitareale, P., and Ciriolo, M. R. Rescue of cells from apoptosis by inhibition of active GSH extrusion. FASEB J., *12:* 479–486, 1998.
8. Filomeni, G., Rotilio, G., and Ciriolo, M. R. Cell signalling and the glutathione redox system. Biochem. Pharmacol., *64: 1059–1066,* 2002.
9. Wargovich, M. J. Experimental evidence for cancer preventive elements in foods. Cancer Lett., *114:* 11–17, 1997.
10. Dong, Y., Lisk, D., Block, E., and Ip, C. Characterization of the biological activity of γ-glutamyl-Se-methylselenocysteine: a novel, naturally occurring anticancer agent from garlic. Cancer Res., *61:* 2923–2928, 2001.
11. Kuwajerwala, N., Cifuentes, E., Gautam, S., Menon, M., Barrack, E. R., and Reddy, G. P. Resveratrol induces prostate cancer cell entry into S phase and inhibits DNA synthesis. Cancer Res., *62:* 2488–2492, 2002.
12. Sheen, L. Y., Wu, C. C., Lii, C. K., and Tsai, S. J. Effect of diallyl sulfide and diallyl disulfide, the active principles of garlic, on the aflatoxin B(1)-induced DNA damage in primary rat hepatocytes. Toxicol. Lett., *122:* 45–52, 2001.
13. Fu, Y. C., Jin, X. P., and Wie, S. M. The effects on cell growth of tea polyphenols acting as a strong anti-peroxidatant and an inhibitor of apoptosis in primary cultured rat skin cells. Biomed. Environ. Sci., *13:* 170–179, 2000.
14. Omkumar, R. V., Kadam, S. M., Banerji, A., and Ramasarma, T. On the involvement of intramolecular protein disulfide in the irreversible inactivation of 3-hydroxy-3-methylglutaryl-CoA reductase by diallyl disulfide. Biochim. Biophys. Acta, *1164:* 108–112, 1993.
15. Gupta, N., and Porter, T. D. Garlic and garlic-derived compounds inhibit human squalene monooxygenase. J. Nutr., *131:* 1662–1667, 2001.
16. Kwon, K. B., Yoo, S. J., Ryu, D. G., Yang, J. Y., Rho, H. W., Kim, J. S., Park, J. W., Kim, H. R., and Park, B. H. Induction of apoptosis by diallyl disulfide through activation of caspase-3 in human leukemia HL-60 cells. Biochem. Pharmacol., *63:* 41–47, 2002.
17. Robert, V., Mouille, B., Mayeur, C., Michaud, M., and Blachier, F. Effects of the garlic compound diallyl disulfide on the metabolism, adherence and cell cycle of HT-29 colon carcinoma cells: evidence of sensitive and resistant sub-populations. Carcinogenesis (Lond.), *22:* 1155–1161, 2001.
18. Sheen, L. Y., Lii, C. K., Sheu, S. F., Meng, R. H., and Tsai, S. J. Effect of the active principle of garlic–diallyl sulfide–on cell viability, detoxification capability and the antioxidation system of primary rat hepatocytes. Food Chem. Toxicol., *34:* 971–978, 1996.
19. Bose, C., Guo, J., Zimniak, L., Srivastava, S. K., Singh, S. P., Zimniak, P., and Singh, S. V. Critical role of allyl groups and disulfide chain in induction of Pi class glutathione transferase in mouse tissues *in vivo* by diallyl disulfide, a naturally occurring chemopreventive agent in garlic. Carcinogenesis (Lond.), *23:* 1661–1665, 2002.
20. Wu, C. C., Sheen, L. Y., Chen, H. W., Tsai, S. J., and Lii, C. K. Effects of organosulfur compounds from garlic oil on the antioxidation system in rat liver and red blood cells. Food Chem. Toxicol., *39:* 563–569, 2001.
21. Ciriolo, M. R., De Martino, A., Lafavia, E., Rossi, L., Carri, M. T., and Rotilio, G. Cu, Zn-superoxide dismutase-dependent apoptosis induced by nitric oxide in neuronal cells. J. Biol. Chem., *275:* 5065–5072, 2000.
22. Perkins, E., Calvert, J., Lancon, J. A., Parent, A. D., and Zhang, J. Inhibition of H-ras as a treatment for experimental brain C6 glioma. Brain. Res. Mol. Brain Res., *111:* 42–51, 2003.
23. Ciriolo, M. R., Aquilano, K., De Martino, A., Carri, M. T., and Rotilio, G. Differential role of superoxide and glutathione in S-nitrosoglutathione-mediated apoptosis: a rationale for mild forms of familial amyotrophic lateral sclerosis associated with less active Cu, Zn superoxide dismutase mutants. J. Neurochem., *77:* 1433–1443, 2001.
24. Filomeni, G., Rotilio, G., and Ciriolo, M. R. Glutathione disulfide induces apoptosis in U937 cells by a redox-mediated p38 MAP kinase pathway. FASEB J., *17:* 64–66, 2003.
25. Nicoletti, I., Migliorati, G., Pagliacci, M. C., Grignani, F., and Riccardi, C. A rapid and simple method for measuring thymocyte apoptosis by propidium iodide staining and flow cytometry. J. Immunol. Methods, *139:* 271–279, 1991.
26. Aquilano, K., Rotolio, G., and Ciriolo, M. R. Proteasome activation and nNOS down-regulation in neuroblastoma cells expressing a Cu, Zn superoxide dismutase mutant involved in familial ALS. J. Neurochem., *85:* 1324–1335, 2003.
27. Lowry, O. H., Rosebrough, N. J., Farr, A. L., and Randall, R. J. Protein measurement with the Folin-phenol reagent. J. Biol. Chem., *193:* 265–275, 1951.
28. Voehringer, D. W., and Meyn, R. E. Redox aspects of Bcl-2 function. Antioxid. Redox Signal., *2:* 537–550, 2000.
29. Liu, R., Li, B., Flanagan, S. W., Oberley, L. W., Gozal, D., and Qiu, M. Increased mitochondrial antioxidative activity or decreased oxygen free radical propagation prevent mutant SOD1-mediated motor neuron cell death and increase amyotrophic lateral sclerosis-like transgenic mouse survival. J. Neurochem., *80:* 488–500, 2002.
30. Ueda, S., Masutani, H., Nakamura, H., Tanaka, T., Ueno, M., and Yodoi, J. Redox control of cell death. Antioxid. Redox Signal., *4:* 405–414, 2002.
31. Adler, V., Yin, Z., Fuchs, S. Y., Benezra, M., Rosario, L., Tew, K. D., Pincus, M. R., Sardana, M., Henderson, C. J., Wolf. C. R., Davis, R. J., and Ronai, Z. Regulation of JNK signaling by GSTp. EMBO J., *18:* 1321–1334, 1999.
32. Goillot, E., Raingeaud, J., Ranger, A., Tepper, R. I., Davis, R. J., Harlow, E., and Sanchez, I. Mitogen-activated protein kinase-mediated Fas apoptotic signaling pathway. Proc. Natl. Acad. Sci. USA, *94:* 3302–3307, 1997.
33. Lea, M. A., and Randolph, V. M. Induction of histone acetylation in rat liver and hepatoma by organosulfur compounds including diallyl disulfide. Anticancer Res., *21:* 2841–2845, 2001.
34. Lea, M. A., Randolph, V. M., and Patel, M. Increased acetylation of histones induced by diallyl disulfide and structurally related molecules. Int. J. Oncol., *15:* 347–352, 1999.
35. Knowles, L. M., and Milner, J. A. Diallyl disulfide inhibits p34(cdc2) kinase activity through changes in complex formation and phosphorylation. Carcinogenesis (Lond.), *21:* 1129–1134, 2000.

36. Knowles, L. M., and Milner, J. A. Possible mechanism by which allyl sulfides suppress neoplastic cell proliferation. J. Nutr., *131:* 1061S–1066S, 2001.
37. Singh, S. V., Mohan, R. R., Agarwal, R., Benson, P. J., Hu, X., Rudy, M. A., Xia, H., Katoh, A., Srivastava, S. K., Mukhtar, H., Gupta, V., and Zaren, H. A. Novel anti-carcinogenic activity of an organosulfide from garlic: inhibition of H-RAS oncogene transformed tumor growth *in vivo* by diallyl disulfide is associated with inhibition of p21H-ras processing. Biochem. Biophys. Res. Commun., *225:* 660–665, 1996.
38. Singh, S. V. Impact of garlic organosulfides on p21(H-ras) processing. J. Nutr., *131:* 1046S–1048S, 2001.
39. Tibbles, L. A., and Woodgett, J. R. The stress-activated protein kinase pathways. Cell. Mol. Life Sci., *55:* 1230–1254, 1999.
40. Herdegen, T., and Waetzig, V. AP-1 proteins in the adult brain: facts and fiction about effectors of neuroprotection and neurodegeneration. Oncogene, *20:* 2424–2437, 2001.
41. Adler, V., Yin, Z., Tew, K. D., and Ronai, Z. Role of redox potential and reactive oxygen species in stress signaling. Oncogene, *18:* 6104–6111, 1999.
42. Buschmann, T., Potapova, O., Bar-Shira, A., Inanov, V. N., Fuchs, S. Y., Henderson, S., Fried, V. A., Minamoto, T., Alarcon-Vargas, D., Pincus, M. R., Gaarde, W. A., Holbrook, N. J., Shiloh, Y., and Ronai, Z. Jun NH2-terminal kinase phosphorylation of p53 on thr-81 is important for p53 stabilization and transcriptional activities in response to stress. Mol. Cell. Biol., *21:* 2743–2754, 2001.
43. Hatai, T., Matsuzawa, A., Inoshita, S., Mochida, Y., Kuroda, T., Sakamaki, K., Kuida, K., Yonehara, S., Ichijo, H., and Takeda, K. Execution of apoptosis signal-regulating kinase 1 (ASK1)-induced apoptosis by the mitochondria-dependent caspase activation. J. Biol. Chem., *275:* 26576–26581, 2000.
44. Schroeter, H., Boyd, C. S., Ahmed, R., Spencer, J. P., Duncan, R. F., Rice-Evans, C., and Cadenas, E. JNK-mediated modulation of brain mitochondria function: New target proteins for JNK signaling in mitochondria-dependent apoptosis. Biochem. J., published on-line: 10.1042/BJ20030201, 2003.
45. Herr, I., and Debatin, K. M. Cellular stress response and apoptosis in cancer therapy. Blood, *98:* 2603–2614, 2001.